Macromolecules

Article

pubs.acs.org/Macromolecules

Core Cross-Linked Multiarm Star Polymers with Aggregation-Induced Emission and Temperature Responsive Fluorescence Characteristics

Zhen Zhang,[†] Panayiotis Bilalis,[†] Hefeng Zhang,[†,§] Yves Gnanou,[‡] and Nikos Hadjichristidis*[,†]

[†]Physical Sciences and Engineering Division, KAUST Catalysis Center, Polymer Synthesis Laboratory and [‡]Physical Sciences and Engineering Division, King Abdullah University of Science and Technology (KAUST), Thuwal 23955, Saudi Arabia

Supporting Information

ABSTRACT: Aggregation-induced emission (AIE) active core cross-linked multiarm star polymers, carrying polystyrene (PS), polyethylene (PE), or polyethylene-*b*-polycaprolactone (PE-*b*-PCL) arms, have been synthesized through an "arm-first" strategy, by atom transfer radical copolymerization (ATRP) of a double styrene-functionalized tetraphenylethene (TPE-2St) used as a cross-linker with linear arm precursors possessing terminal ATRP initiating moieties. Polyethylene macroinitiator (PE−Br) was prepared via the polyhomologation of dimethylsulfoxonium methylide with triethylborane followed by oxidation/hydrolysis and esterification of the produced PE−OH with 2-bromoisobutyryl bromide; polyethylene-*block*-poly(ε-caprolactone) diblock macroinitiator was derived by combining polyhomologation with ring-opening polymerization (ROP). All synthesized star polymers showed AIE-behavior either in solution or in bulk. At high concentration in good solvents (e.g., THF, or toluene) they exhibited low photoluminescence (PL) intensity due to the inner filter effect. In sharp contrast to the small molecule TPE-2St, the star polymers were highly emissive in dilute THF solutions. This can be attributed to the cross-linked structure of poly(TPE-2St) core which restricts the intramolecular rotation and thus induces emission. In addition, the PL intensity of PE star polymers in THF(solvent)/*n*-hexane(nonsolvent) mixtures, due to their nearly spherical shape, increased when the temperature decreased from 55 to 5 °C with a linear response in the range 40−5 °C.

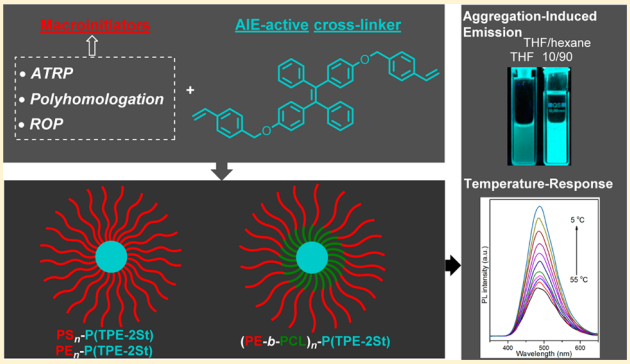

INTRODUCTION

Luminescent materials have attracted strong interest in recent decades due to their significant applications in electronic and bioimaging areas.[1−4] The conventional luminophores experience high emission in dilute solution, but undergo partial or complete light emission quenching when aggregated.[5] This undesirable aggregation-caused quenching (ACQ) effect hinders the practical use of luminescent materials in solid or aggregated state. In contrast, propeller-like molecules, e.g. tetraphenylethene (TPE), are nonluminescent in dilute solution but emissive in aggregated state. This exactly opposite phenomenon of ACQ was discovered and documented as aggregation-induced emission (AIE) by Tang in 2001.[6,7] The restriction of intramolecular rotation (RIR) in the aggregate state leads to the radiative decay of excitations, which has been identified as the main cause for the AIE effect.[8] In contrast, active rotations of peripheral phenyl rings effectively annihilate the exited states in dilute solution. Until now, many new AIE molecules have been designed/synthesized and applied in chemosensing, bioimaging, optoelectronics, stimuli-responsive systems, and so on.[9−11]

To achieve facile fabrication of thin films and devices, AIE-active polymers have been largely explored.[12] Owing to the unique structures or chemical compositions, AIE properties can be combined with polymer properties to obtain emission in response to external stimuli such as heat,[13,14] pH,[15] light,[16] chemicals,[17] etc. For example, Tang and co-workers synthesized a hyperbranched poly(silylenephenylene) which acts as as a highly sensitive chemosensor for detection of explosives with a super amplification effect due to the three-dimensional (3D) structure.[18,19] Taniguchi et al. synthesized TPE cross-linked poly(dimethylsiloxane) (PDMS) elastomers through the hydrosilylation reaction of tetravinyl-modified TPE derivative and H-terminated PDMS.[20] Such AIE elastomers exhibited stimuli-sensitive behavior in organic solvents with the extent of swelling influenced by the nature of the solvent used. Studies have not only focused on hyperbanched and cross-linked polymers but also linear, star, dendritic, microporous, and supermolecular polymers have been investigated and their remarkable properties reported.[21] However, in most cases, the reported AIE polymers are nonemissive or weakly fluorescent when dissolved in their good solvents, a typical AIE feature.[18] The applications

Received: March 8, 2017
Revised: May 15, 2017

DOI: 10.1021/acs.macromol.7b00506
Macromolecules XXXX, XXX, XXX−XXX

of AIE luminogens are thus limited in aggregate state. To further promote their potential applications, developing AIE systems or synthesizing AIE polymers with AIE effect not only in aggregate state but also in good solvent is a challenging topic.

Although star polymers, carrying AIE moieties either in the core or in the arms have already reported,[22−24] stars with a cross-linked AIE core have never been synthesized/investigated until now. Furthermore, the ATRP "arm-first" strategy, developed by Matyjaszewski, Sawamoto, Chen, Qiao, et al. for a variety of styrenic and (meth)acrylic star polymers,[25−31] was applied only in one case of PE stars. The ATRP of divinylbenzene was initiated by 2-bromoisobutyryl end-capped and branched PE-macroinitiators, the latter being synthesized by Pd-catalyzed polymerization of ethylene.[32−34]

In contrast to the polymerization of ethylene by coordination metal complexes, polyhomologation, an organoborane-initiated polymerization of dimethylsulfoxonium methylide,[34] has been proven as an efficient tool to synthesize well-defined and perfectly linear hydroxyl-terminated polymethylene (PE analogue), as well as other PE-based architectures in combination with other polymerization techniques.[35−40] Recently, we developed a "core-first" strategy by using a functionalized B-thexylboracycle initiator for the synthesis of 4-arm star PE and in combination with ATRP for the synthesis of PE-based 3-miktoarm stars.[41−43]

Herein, we wish to report the synthesis via "arm-first" strategy of core cross-linked multiarm stars made of polystyrene (PS), polyethylene (PE) or polyethylene-*b*-poly(ε-caprolactone) (PE-*b*-PCL) arms, and a cross-linked TPE-2St core. The cross-linking reaction was carried out by ATRP, using TPE-2St as cross-linker and the above-mentioned Br-terminated precursors as macroinitiators. These macroinitiators were themselves synthesized by ATRP, polyhomologation and ROP. As the rigid cross-linked structure of P(TPE-2St) core significantly inhibited the intramolecular motions of TPE's phenyls, the synthesized star polymers were highly emissive not only in the aggregate state but also in the dilute solutions. Because of the highly compact nanoscale three-dimensional globular structure, the star polymers exhibited temperature responsive fluorescence.

EXPERIMENTAL SECTION

Materials. 4-Hydroxybenzophenone (98%), zinc powder, titanium tetrachloride ($TiCl_4$, ≥ 98%), 4-vinylbenzyl chloride (90%), potassium carbonate (anhydrous, ≥ 99.0%), copper(I) bromide (CuBr, 99.999%), *N*,*N*,*N*′,*N*″,*N*″-pentamethyldiethylenetriamine (PMDETA, 99%), triethylborane solution (1.0 M in THF), trimethylamine *N*-oxide dihydrate (TAO·$2H_2O$) (≥99%), ethyl α-bromoisobutyrate (98%), phosphazene base P2-*t*Bu solution (~2 M in THF), 2-bromoisobutyryl bromide (BIBB, 98%), and pyridine (99.8%) were purchased from Aldrich and used as received. Styrene (St, ≥ 99%), and ε-caprolactone (CL, 97%) were distilled over calcium hydride (CaH_2) under reduced pressure. Tetrahydrofuran (THF) and toluene were refluxed over sodium/benzophenone and distilled under a nitrogen atmosphere just before use. Acetonitrile (CH_3CN) was used as received. Dimethylsulfoxonium methylide was prepared according to the Corey's method followed by switching the solvent from THF to toluene.[44] PS−Br was prepared according to the typical ATRP procedure initiated by ethyl α-bromoisobutyrate with CuBr/PMDETA as catalyst.[45]

Measurements. The ^1H and ^{13}C NMR spectra were recorded with a Bruker AVANCE III-400, 500, or 600 spectrometer. The molecular weight ($M_{n,GPC}$) and molecular weight distribution ($Đ$) of linear and star polystyrenes were measured by gel permeation chromatography (GPC) (Viscoteck 305 instrument with two columns of Styragel HR2 and Styragel HR4) with THF eluent at 35 °C, flow rate =1.0 mL/min and differential refractive index (RI) detector. For PE-based linear and star polymers, $M_{n,GPC}$ and $Đ$ were measured on a Viscoteck high temperature gel permeation chromatography (HT-GPC) module 350 instrument with two PLgel 10 μm MIXED-B columns and 1,2,4-trichlorobenzene (TCB) as the eluent at a flow rate of 0.8 mL/min at 150 °C. The absolute molecular weight ($M_{w,GPC-LS}$) of star polymers and $Đ_{GPC-LS}$ were determinted by triple-detection GPC or HT-GPC (refractometry, light scattering at λ = 670 nm and viscometry). Both GPCs were calibrated with PS standard ($M_w = 115 \times 10^3$ g/mol, $Đ$ = 1.05). DSC measurements were performed using a Mettler Toledo DSC1/TC100 system under inert atmosphere (nitrogen). The sample was heated from room temperature to 150 °C, cooled to −10 °C and finally heated again to 150 °C with a heating/cooling rate of 10 °C/min. The second heating curve was used to determine the glass transition temperature (T_g) and melting temperature (T_m). Transmittance measurements were performed on a Thermo Evolution 600 UV−vis spectrophotometer equipped in quartz cuvettes of 10 mm path length at a wavelength of 500 nm at room temperature. Photoluminescence spectra were recorded on a Thermo Lumina fluorescence spectrometer equipped an external water circulator for the thermostated cell holder. Dynamic light scattering (DLS) measurements were made with a Brookhaven BI-200SM multiangle goniometer with a TurboCorr correlator. The light source was a 30 mW He−Ne laser emitting vertically polarized light of 632.8 nm wavelength.

Synthesis of Cross-Linker 1,2-Diphenyl-1,2-bis(4-((4-vinylbenzyl)oxy)phenyl)ethane (TPE-2St). Zn powder (11.6 g, 0.18 mol) and 4-hydroxybenzophenone (8.0 g, 0.040 mol) were placed into a 250 mL two-necked flask equipped with a condenser. The flask was evacuated under vacuum and flashed with argon three times, followed by addition of anhydrous THF (200 mL). Then the mixture was cooled to −78 °C and $TiCl_4$ (10.0 mL, 0.18 mol) was added dropwise. The mixture was slowly warmed to room temperature, stirred for 30 min, and then refluxed overnight. After cooling down to room temperature, the reaction was quenched by 10% aqueous K_2CO_3 solution, and after vigorous stirring for 5 min, the dispersed insoluble material was removed by vacuum filtration using a Celite pad. The organic phase was separated and the aqueous layer was extracted three times with diethyl ether (60 mL × 3). The combined organic fractions were washed with saturated NaCl solution and dried over $MgSO_4$. The solvent was removed to give the crude 4,4′-(1,2-diphenylethene-1,2-diyl)diphenol (TPE-2OH).[46]

Without purification, the crude TPE-2OH was dissolved in acetonitrile (150 mL). Then K_2CO_3 (0.20 mol, 28 g) and 4-vinylbenzyl chloride (0.060 mol, 9.3 mL) were added under argon, and the mixture refluxed for 5 h. After filtration and removal of solvent, the residue was chromatographed over silica gel (dichloromethane/petroleum ether: 1/5) to give main product *E*-TPE-2St as white solid (8.3 g, 70% yield in two steps). *E*-TPE-2St: ^1H NMR (500 MHz, $CDCl_3$) δ 4.96 (s, 4H), 5.27 (2H, d, *J* = 10.0 Hz), 5.78 (2H, d, *J* = 20.0 Hz), 6.71−6.77 (6H, m), 6.93−6.95 (3H, m), 7.04−7.15 (10H, m), 7.36−7.37 (3H, m), 7.42−7.44 (4H, m). ^{13}C NMR (100 MHz, $CDCl_3$) δ 69.6, 113.9, 114.0, 114.1, 126.2, 126.3, 127.5, 127.8, 131.4, 132.5, 136.4, 136.5, 136.7, 137.3, 139.7, 144.1, 157.2. HRMS (ESI): calcd for $C_{44}H_{37}O_2$ $[M + H]^+$, *m*/*z* 597.2794; found, *m*/*z* 597.2766.

Synthesis of Linear Polyethylene Macroinitiator PE−Br. PE−OH was prepared according to Shea's work.[36] A 500 mL flask, charged with dimethylsulfoxonium methylide solution (165 mL, 0.6 M in toluene), was heated to 60 °C with stirring under argon. Then triethylborane solution (0.4 mL, 1.0 M in THF) was rapidly injected via syringe. After 10 min, a drop of the mixture was taken out and added to water containing phenolphalein. The neutral solution indicated the complete consumption of the ylide. Then TAO·$2H_2O$ (0.80 g) was added, and the reaction stirred at 80 °C for 5 h. The mixture was concentrated and poured into cold methanol (300 mL). Filtration of the precipitate, washing with methanol, and drying under vacuum afforded a white solid (1.3 g, $M_{n,NMR}$ = 1460, $M_{n,theor}$ = 1260, $Đ$ = 1.15). ^1H NMR (600 MHz, $CDCl_2CDCl_2$, 90 °C): δ 0.91−0.96

DOI: 10.1021/acs.macromol.7b00506
Macromolecules XXXX, XXX, XXX−XXX

Scheme 1. Reaction Steps for the Synthesis of Cross-Linker TPE-2St

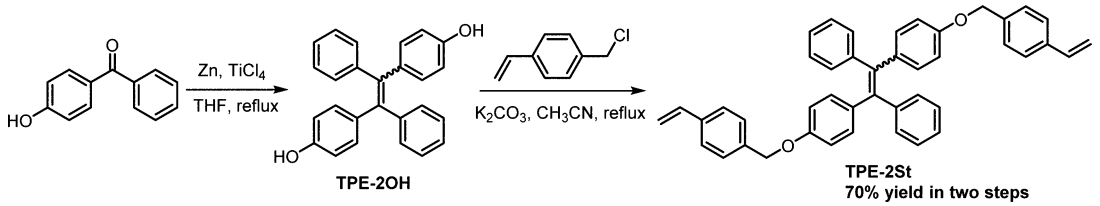

Scheme 2. Synthetic Routes for Macroinitiators (a) PS−Br, (b) PE−Br, and (c) TBDMSO-PE-*b*-PCL−Br and Core Cross-Linked Multiarm Star Polymers (d) $(PS)_n$-P(TPE-2St) or $(PE)_n$-P(TPE-2St) and (e) $(TBDMSO\text{-}PE\text{-}b\text{-}PCL)_n$-P(TPE-2St)

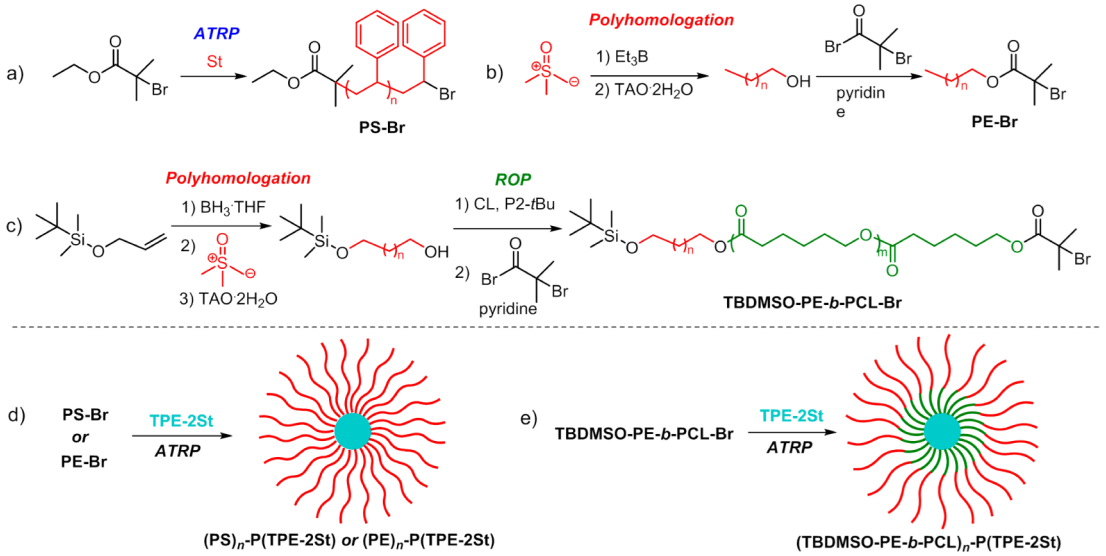

(9H, m), 1.34 (204H, brs), 1.59−1.63 (2H, m), 3.66 (2H, t, J = 6.0 Hz).

PE−OH (1.0 g, 0.68 mmol of OH) and toluene (40 mL) were placed into a 100 mL Schlenk flask and the mixture was kept under vigorous stirring at 100 °C under Ar. Pyridine (0.49 mL, 6.0 mmol) and 2-bromoisobutyryl bromide (0.90 mL, 7.2 mmol) were added dropwise. After being stirred for 12 h, the reaction mixture was cooled to room temperature and poured into 300 mL of acidic methanol (containing 30 mL of 1 M aqueous HCl). The solid was filtered, washed successively with methanol (2 × 20 mL), 1 M aqueous HCl (2 × 10 mL), and methanol (2 × 20 mL), and dried at 50 °C for 3 h in vacuum to give an off-white solid (0.80 g, $M_{n,NMR}$ = 1610, $Đ$ = 1.16). ^{1}H NMR (600 MHz, $CDCl_2CDCl_2$, 90 °C): δ 0.90−0.95 (9H, m), 1.33 (204H, brs), 1.70−1.75 (2H, m), 1.97 (6H, s), 4.21 (2H, t, J = 6.0 Hz).

Synthesis of Linear Diblock Macroinitiator TBDMSO-PE-*b*-PCL−Br. As described in our previous work, TBDMSO-PE−OH (TBDMSO-: *tert*-butyldimethylsilyoxyl) was prepared from allyl alcohol via three steps including protection of allyl alcohol, hydroboration and polyhomologation reactions.[39] Then ring-opening polymerization of ϵ-caprolactone with TBDMSO-PE−OH as macroinitiator and phosphazene base P2-*t*Bu as catalyst, TBDMSO-PE-*b*-PCL−OH was obtained.[43] TBDMSO-PE-*b*-PCL−OH was converted to TBDMSO-PE-*b*-PCL−Br by reacting with 2-bromo-2-methylpropionyl bromide in the presence of pyridine in toluene at 100 °C as more details described above.

Synthesis of Core Cross-Linked Multiarm Star Polymers. As an example the synthesis of $(PE)_{136}$-P(TPE-2St) star is given. CuBr (14 mg, 0.10 mmol), TPE-2St (0.60 g, 1.0 mmol), PE−Br (0.16 g, 0.10 mmol, $M_{n,NMR}$ = 1610), and toluene (6.0 mL) were placed into a 100 mL Schlenk flask. The mixture was subjected to three freeze−pump−thaw cycles and then PMDETA (42 μL, 0.20 mmol) was added and the mixture was subjected to another one freeze−pump−thaw cycle. The solution was immediately immersed into an oil bath set at 100 °C to start the polymerization under stirring. After 25 h, the polymerization was stopped by cooling in a liquid nitrogen bath. The cloudy solution was diluted with toluene (~5 mL), heated to clear and poured into cold methanol (300 mL) with stirring. The solid was filtered, washed with methanol, dried under vacuum, and characterized by ^{1}H NMR and HT-GPC (0.60 g, $M_{n,GPC\text{-}LS}$ = 875.5 × 10^3, $Đ_{GPC\text{-}LS}$ = 2.38).

The synthetic procedures of $(PS)_n$-P(TPE-2St) and P(TBDMSO-PE-*b*-PCL)$_n$-P(TPE-2St) were similar to that of $(PE)_{136}$-P(TPE-2St).

RESULTS AND DISCUSSION

Cross-Linker: Synthesis and Photoluminescence. The AIE cross-linker TPE-2St was synthesized according to the steps shown in Scheme 1.

The first step was the McMurry coupling reaction of 4-hydroxybenzophenone to afford dihydroxyl functionalized tetraphenylethylene (TPE-2OH). Crude TPE-2OH can be used for the next step without purification. The second step was the Williamson ether reaction between the hydroxyl groups of TPE-2OH and 4-vinylbenzyl chloride which afforded tetraphenylethylene having two styrene groups (TPE-2St) (70% final yield in the two steps). To avoid the contamination of TPE-2St with unreacted 4-vinylbenzyl chloride, it was carefully purified by silica gel chromatography.

The photoluminescence (PL) of TPE-2St in THF and THF/H_2O mixtures was investigated (Figure S1, Supporting Information). For TPE molecule, the restriction of intramolecular rotation (RIR) of the phenyl rotors in the aggregates has been demonstrated experimentally and theoretically as the main source for the AIE effect.[47−51] Thus, only a slight fluorescent signal at 474 nm could be detected in dilute THF solution or in aqueous mixtures with f_w 0−70% water content.

DOI: 10.1021/acs.macromol.7b00506
Macromolecules XXXX, XXX, XXX−XXX

Table 1. Molecular Characterization Results of Linear Macroinitiators (MIs)

entry	MI	$M_{n,NMR}$ (kg/mol)[a]	DP[a]	$M_{n,GPC}$ (kg/mol)[b]	$Đ$[b]
1	PS−Br	5.7	54	6.8	1.09
2	PE−Br-1	2.5	166	6.4	1.11
3	PE−Br-2	1.6	103	1.2	1.16
4	TBDMSO-PE-*b*-PCL−Br[c]	6.6	108, 45[d]	7.2	1.23

[a]$M_{n,NMR}$ and degree of polymerization (DP) were calculated from ^{1}H NMR spectra. [b]$M_{n,GPC}$, $Đ = M_w/M_n$, determined by GPC (for PS−Br: THF, 35 °C, PS standards; for PE−Br and TBDMSO-PE-*b*-PCL−Br, trichlorobenzene, 150 °C, PS standards). [c]TBDMSO-: *tert*-butyldimethylsilyoxyl. [d]DP_{PE} = 108; DP_{PCL} = 45

Table 2. ATRP Reaction Conditions and Molecular Characteristics of Synthesized Core Cross-Linked Star Polymers[a]

entry	MI	[MI] (mM)	time (h)	[TPE-2St]:[MI]	$M_{n,RI}$ (kg/mol)[b]	$Đ_{RI}$[b]	$M_{w,GPC-LS}$ (kg/mol)[c]	$Đ_{GPC-LS}$[c]	R_h (nm)[c]	N_{arm}[d]
1	PS−Br	27.5	22	10:1	gel					
2	PS−Br	20.0	22	10:1	40.9	1.77	661.7	2.20	11.5	54.9
3	PS−Br	12.5	64	5:1	37.0	1.37	128.8	1.84	8.4	14.3
4	PE−Br-1	12.5	65	10:1	36.8	1.21	[e]	[e]	[e]	[e]
5	PE−Br-2	16.7	25	10:1	26.4	2.36	875.5	2.38	11.1	136
6	PE−Br-2	16.7	25	13:1	25.1	2.92	2008	2.01	14.6	262
7	TBDMSO-PE-*b*-PCL−Br	12.5	22	13:1	93.9	1.97	[e]	[e]	[e]	[e]
8	TBDMSO-PE-*b*-PCL−Br	12.5	23	10:1	[e]	[e]	[e]	[e]	[e]	[e]

[a]Polymerization conditions: toluene, 90 °C, [CuBr]:[PMDETA]:[MI] = 1:2:1. [b]$M_{n,RI}$ and $Đ_{RI}$, determined by GPC (entries 2 and 3) or HT-GPC (entries 4−7) RI detector. [c]$M_{w,GPC-LS}$, $Đ_{GPC-LS}$ and R_h (hydrodynamic radius) determined by triple-detection GPC (entries 2 and 3) or HT-GPC (entries 5 and 6). [d]Average number of arms: $N_{arm} = (M_{W,star} \times arm_{wt\ \%})/M_{n,NMR,arm}$. [e]Not measured due to the poor solubility.

When a large amount of water was added into the THF solution the emission intensity was boosted to ∼75-fold (f_w = 80%), and to ∼300-fold (f_w = 90%) of that of pure THF solution, caused by the aggregation and the resulting restriction in intramolecular rotation.

Macroinitiators. Different kinds of linear macroinitiators were synthesized via living and controlled/living polymerization techniques. PS macroinitiator (PS−OH) was prepared through ATRP of styrene initiated by ethyl α-bromoisobutyrate (Scheme 2a). Polyhomologation of dimethylsulfoxonium methylide initiated by triethylborane led to hydroxyl terminated PE, which was converted to PE−Br ATRP macroinitiator by esterification using 2-bromoisobutyryl bromide (Scheme 2b). TBDMSO-PE−OH was prepared via polyhomologation reaction initiated by tri[3-(*tert*-butyldimethylsilyloxyl)propyl]-borane,[39] followed by ring-opening polymerization of ε-caprolactone from TBDMSO-PE−OH as macroinitiator and phosphazene base P2-*t*Bu as catalyst. TBDMSO-PE-*b*-PCL−OH was further transformed to ATRP macroinitiator TBDMSO-PE-*b*-PCL−Br by reaction with 2-bromoisobutyryl bromide (Scheme 2c). The ^{1}H NMR and GPC/HT-GPC characterization results, summarized in Table 1, show the well-defined nature of all synthesized macroinitiators.

Core Cross-Linked Star Polymers. The general conditions allowing the synthesis of core cross-linked multiarm star polymers $(PS)_n$-P(TPE-2St), $(PE)_n$-P(TPE-2St), and $(TBDMSO\text{-}PE\text{-}b\text{-}PCL)_n$-P(TPE-2St) are shown in Scheme 2d and 2e.

Initially, PS−Br was chosen as model macroinitiator to investigate the reactivity of TPE-2St in the "arm-first" methodology. The concentration of PS−Br was found to have a significant impact on the extent of star formation. Gelation occurred after 22h for a macroinitiator concentration of 27.5 mM and a cross-linker to macroinitiator ratio of 10:1 (Table 2, entry 1). Upon decreasing the PS−Br concentration from 27.5 to 20.0 mM, a soluble star polymer was obtained with a molecular weight of 661.7 kg/mol (determined with triple-detection GPC) and average number of arms (N_{arm}) 54.9 after 22 h reaction (Table 2, entry 2; for GPC traces and NMR spectra, see Figure S2 and S3). The weight fraction of PS arms ($arm_{wt\ \%}$) was determined by ^{1}H NMR. The average number of arms of the star polymer was calculated using the following equation: $N_{arm} = (M_{W,star} \times arm_{wt\ \%})/M_{n,NMR,arm}$. By decreasing further the macroinitiator concentration to 12.5 mM and with a cross-linker to macroinitiator ratio of 5:1, longer time (65 h) was needed to form a soluble star polymer which exhibited a molecular weight of 128.8 kg/mol and a N_{arm} of 14.3 (Table 2, entry 3; for GPC traces, see Figure S4).

Upon using the same initial concentration of 12.5 mM for PE−Br macroinitiator, it was found that most of the PE−Br remained unreacted and subsequent separation of the star polymer from the linear PE was difficult (Table 2, entry 4 and Figure S5). However, upon increasing the MI concentration from 12.5 to 16.7 mM, PE star polymers with different molecular weights (875.5 kg/mol and 2008 kg/mol) could be successfully synthesized, under different TPE-2St to MI ratios (10:1 and 13:1, respectively) (Table 2, entry 5 and 6). From the GPC traces it is evident that most of the PE−Br was consumed and the star polymer was monomodal (Figure 1). As shown in the ^{1}H NMR spectra (Figure 2), both signals due to PE arms and P(TPE-2St) core could be identified. Two other star polymers were synthesized from linear diblock MI TBDMSO-PE-*b*-PCL−Br, but their absolute molecular weights could not be determined by triple detection GPC due to the weak RI signal and poor solubility (Table 2, entry 7 and 8; Figure S6). As shown in Figure 3, star-block copolymers could also be successfully synthesized, as indicated by the signals corresponding to poly(TPE-2St), PE and PCL in the ^{1}H NMR spectra.

DSC Characterization. The DSC traces for the linear PE, PE-*b*-PCL macroinitiators and for the corresponding star polymers are shown in Figure 4. The linear PE with $M_{n,NMR}$ 1600 exhibited a melting temperature (T_m) of 109 °C. For $(PE)_{136}$-P(TPE-2St) star polymer, the melting endotherm due

DOI: 10.1021/acs.macromol.7b00506
Macromolecules XXXX, XXX, XXX−XXX

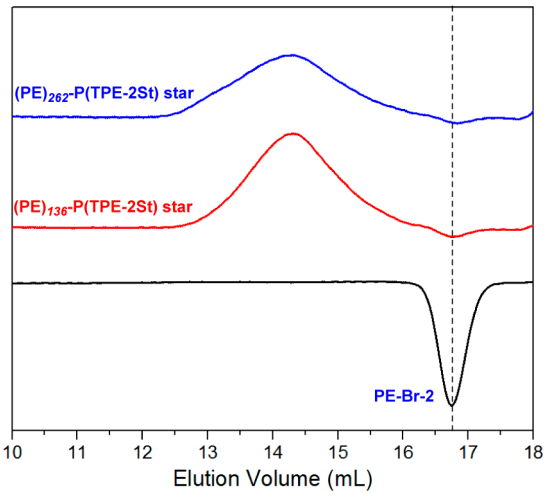

Figure 1. HT-GPC (TCB at 150 °C) traces of linear PE−Br-2 and $(PE)_{136}$-P(TPE-2St), $(PE)_{262}$-P(TPE-2St) stars. (The negative peak of PE−Br-2 is due to the negative DRI of PE.)

to PE segments at 109 °C almost disappeared. With nearly double the number of arms, the melting endotherm vanished for $(PE)_{262}$-P(TPE-2St). Because of the increasing steric crowding in the PE shell, caused by an increased number of arms, the segmental mobility of the PE chains is reduced.[32] In the case of TBDMSO-PE-*b*-PCL−Br, two melting points at 55 and 109 °C were found corresponding to the PCL and PE chains, respectively. For the first PE-*b*-PCL star polymer (sample of Table 2, entry 7), a broad melting endotherm in a temperature range of 74 to 104 °C with a peak at 93 °C was observed along with a weak glass transition at 123 °C. For another sample (sample of Table 2, entry 8), only a broad peak range from 75 to 106 °C with T_m equal to 98 °C was found. Indicated by the disappearance of the melting endotherm in both samples, steric crowding probably prevented the movements of chains which in turn prevented the PCL segments from crystallizing. On the other hand, the PE arms of (PE-*b*-PCL)s are in the periphery and not as sterically hindered as the arms of PCL, but their flexibility and regularity were reduced, which resulted in a lower T_m. Considering the highly restricted mobility of cross-linked core, the observed high T_g could be attributed to the $P(TPE\text{-}2St)_n$ core. In the case of $(PS)_{14.3}$-P(TPE-2St) (T_g: 106 °C) and $(PS)_{54.9}$-P(TPE-2St) (T_g: 110 °C), the glass transition of PS segments shifted to higher temperatures in comparison to that of linear PS−Br (T_g: 96 °C) due to the increase of arm number and resulting reduced mobility (Figure S7).

Aggregation-Induced Emission. The emission character of the solutions of the synthesized star polymers was then investigated. As shown in Figure 5, parts a and b, one of the sample investigated [$(PE)_{136}$-P(TPE-2St)] was weakly emissive with an almost flat peak in the emission spectra at the concentration of 0.001 g/L in THF. When the concentration increased from 0.001 to 0.1 g/L, the emission intensity at λ_{em} = 484 nm gradually increased by ~53.1-fold compared to the initial intensity (0.001 g/L). Unexpectedly, the emission

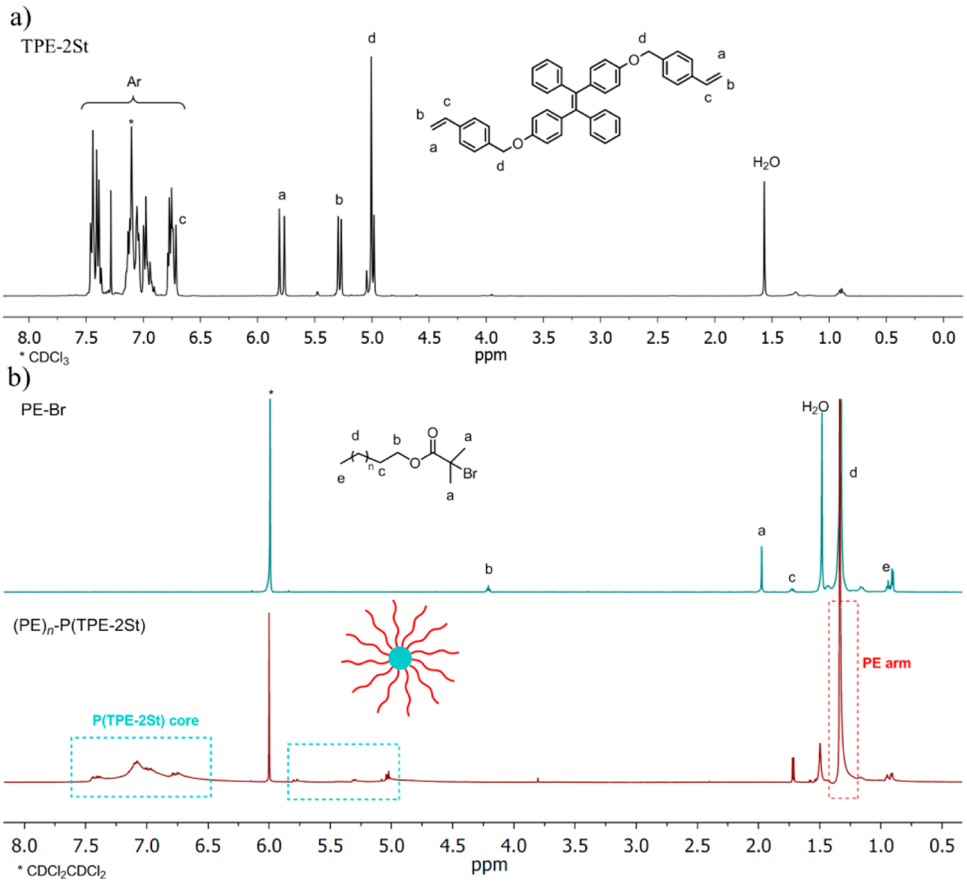

Figure 2. ^1H NMR (600 MHz) spectra of (a) TPE-2St in chloroform-*d* at 25 °C and (b) PE−Br and $(PE)_n$-P(TPE-2St) in 1,1,2,2-tetrachloroethane-d_2 at 90 °C.

DOI: 10.1021/acs.macromol.7b00506
Macromolecules XXXX, XXX, XXX−XXX

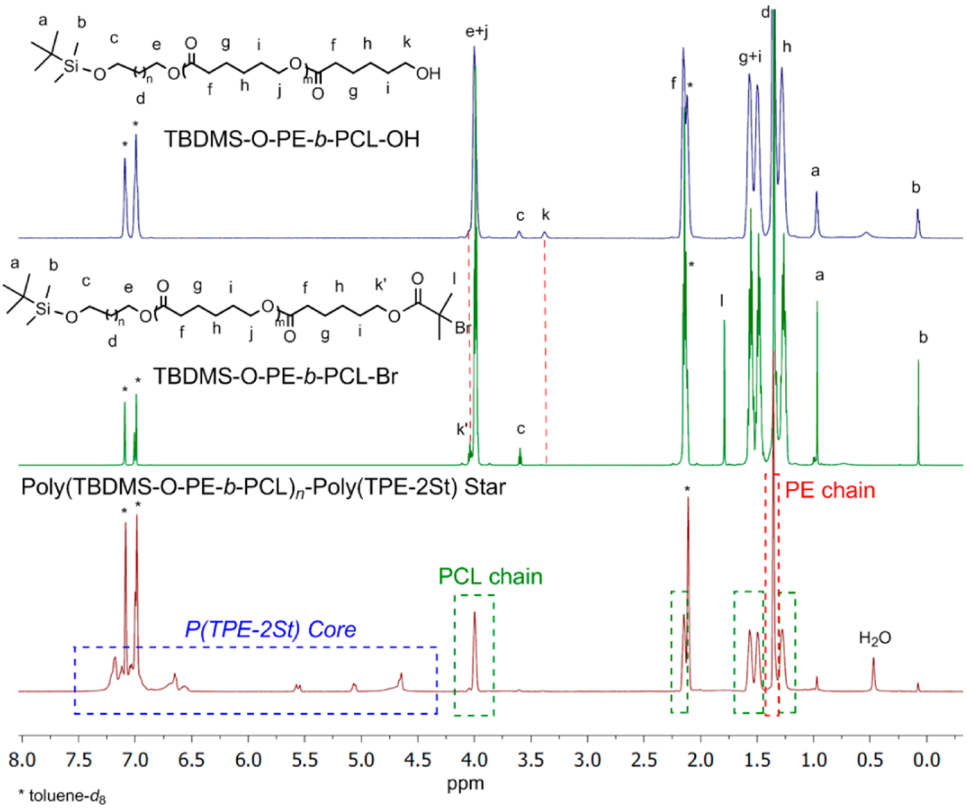

Figure 3. ^{1}H NMR (600 MHz) spectra of TBDMSO-PE-*b*-PCL−OH, TBDMSO-PE-*b*-PCL−Br, and (TBDMSO-PE-*b*-PCL)$_n$-P(TPE-2St) in toluene-d_8 at 90 °C.

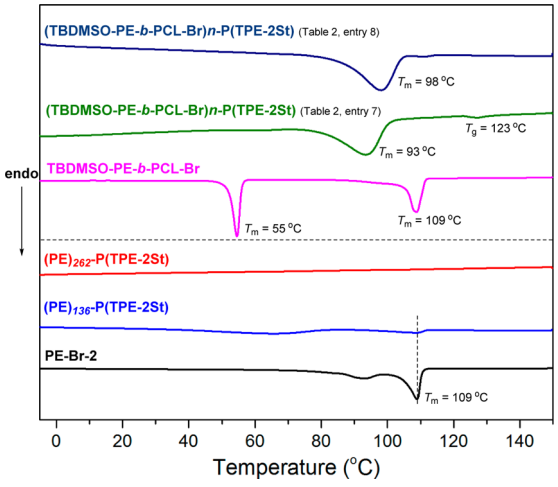

Figure 4. DSC thermograms of synthesized PE-based macroinitiators and star polymers.

intensity dropped to 14% of the highest intensity (0.1 g/L) upon increasing the concentration further from 0.1 to 1 g/L. Emission intensities remained in a range between 14 and 20% of the highest intensity for concentrations ranging from 1 to 5 g/L. Moreover, the transmittance of the solution dropped from 100% to ∼80% when the concentration increased from 0.1 to 1 or 2 g/L. Less than 30% transmittance was observed in the solutions with concentrations ≥3 g/L which can be attributed to the poor solubility of PE arms in THF.

As reported by Tang, poly(naphthopyran)s with TPE units anchored on the backbone underwent "ACQ" in the aggregated state.[52] To clarify if it was indeed "ACQ" or not at high concentration, the emission character of the (PE)$_{136}$-P(TPE-2St) toluene solution was investigated, since the star polymer had a good solubility in toluene (Figure S8). A similar tendency in toluene was observed as in THF. The same phenomenon was also found for another sample (PS)$_{54.9}$-P(TPE-2St) exhibiting a good solubility in THF (Figure S9). DLS results revealed only a slight shift of the mean diameter once the concentration increased (Figure S9). Thus, the aggregation is not the reason for the emission quenching. Moreover, it was observed that only the top layer of the high concentration solution exhibited a strong emission under UV as illustrated in the photos of Figure 5c, S8, and S9, and other parts of the solution had slight emission since the excitation light was incapable of reaching these sites. Hence, the most possible reason is the inner filter effect because of the high concentrations of absorbing molecules.[53] The intensity of the excitation light is not constant through the polymer solution and only a small percentage of the excitation light reaches the TPEs that are visible for the detection system.[54]

To avoid the detrimental inner filter effect, dilute rather than high concentration solutions should be employed to study the photophysical properties of the star polymer solutions. Thus, the AIE behaviors of (PE)$_{136}$-P(TPE-2St) were investigated in dilute THF (solvent)/*n*-hexane(nonsolvent) mixture with a concentration of 0.1 g/L. As shown in parts a and b of Figure 6, addition of *n*-hexane into the THF solution induced the molecules to aggregate and gradually enhanced its PL intensities. The highest emission intensity was observed in 90 vol % mixtures and its intensity enhanced about 5.6-fold compared with that of its THF solution. When the volume content of *n*-hexane ranged from 0 to 70%, the transmittance of the solution stayed the same as 100% which is an indication of

DOI: 10.1021/acs.macromol.7b00506
Macromolecules XXXX, XXX, XXX−XXX

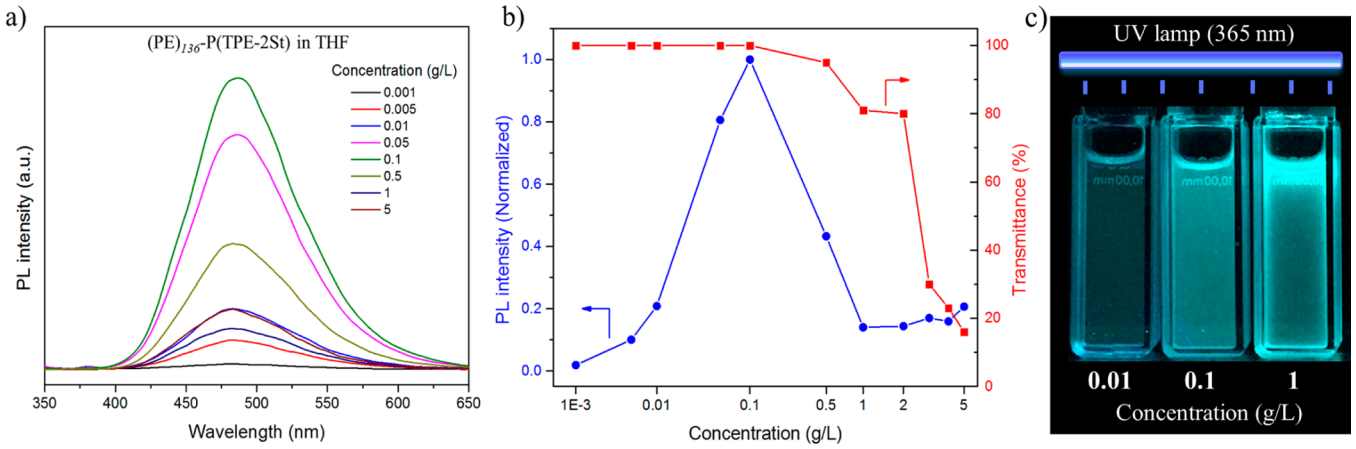

Figure 5. (a) Photoluminescence (PL) spectra of $(PE)_{136}$-P(TPE-2St) in THF at different concentrations as indicated measured at room temperature. (b) Plot of normalized PL intensity and transmittance versus concentration. (c) Photographs of $(PE)_{136}$-P(TPE-2St) in THF at 0.01, 0.1, and 1 g/L concentrations with UV irradiation (365 nm) from the top.

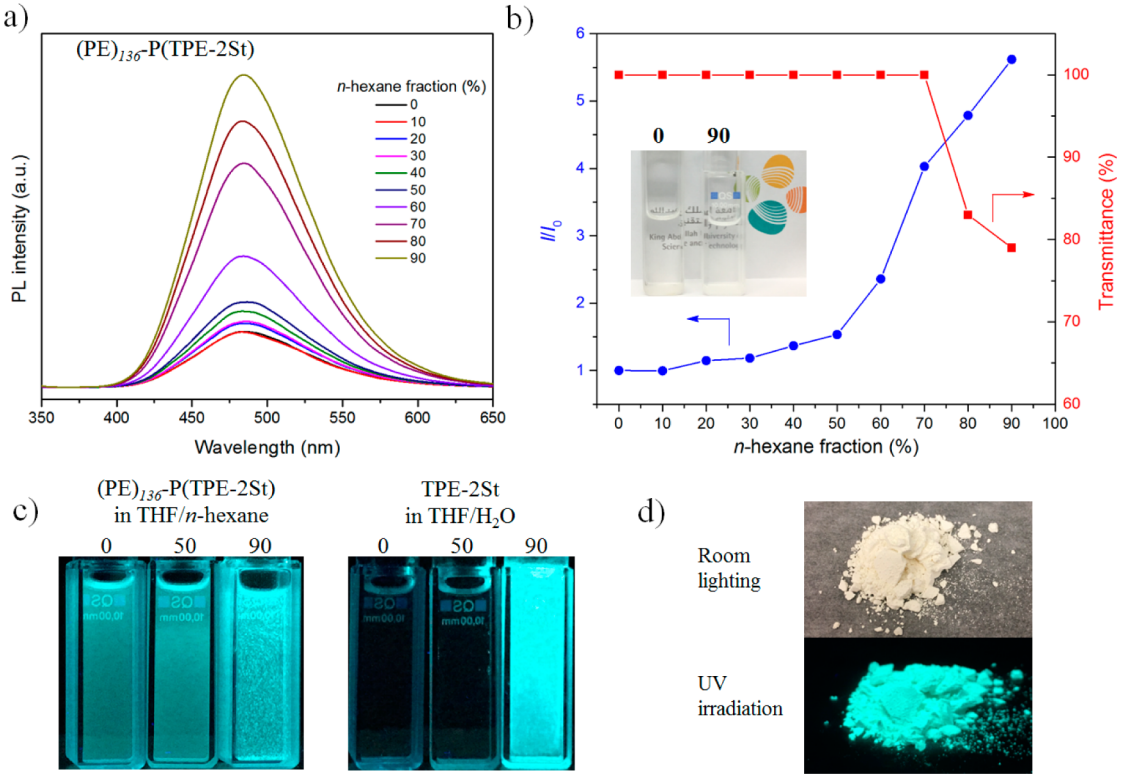

Figure 6. (a) Photoluminescence (PL) spectra of $(PE)_{136}$-P(TPE-2St) in THF/*n*-hexane mixtures with different *n*-hexane fractions at a concentration of 0.1 g/L. (b) Plot of I/I_0 and transmittance *versus* *n*-hexane fraction in the THF/*n*-hexane mixture; I is PL intensity in THF/*n*-hexane mixtures with different *n*-hexane fractions, I_0 is PL intensity in pure THF solution (inset: photographs of THF/*n*-hexane mixtures of polymer with 0 and 90 vol % *n*-hexane fractions taken under room light). (c) Photographs of THF/*n*-hexane mixtures of $(PE)_{136}$-P(TPE-2St), and THF/H_2O mixtures of TPE-2St with 0, 50, and 90 vol % *n*-hexane or H_2O fractions at a concentration of 0.1 g/L taken under 365 nm UV illumination. (d) Images of solid powder of $(PE)_{136}$-P(TPE-2St) taken under room light and under 365 nm UV irradiation.

good solubility of PE star in the THF/*n*-hexane mixture. Transmittance 83% was observed in 80 vol % of *n*-hexane, and 79% transmittance in 90 vol % of *n*-hexane, along with the increase of PL intensity as the PE star aggregated.

It is noteworthy that a strong emission was observed from the $(PE)_{136}$-P(TPE-2St) in pure THF or in THF/*n*-hexane mixtures with low fraction of the nonsolvent *n*-hexane. In sharp contrast, small molecular luminogen TPE-2St displayed high emission only with a large amount of water (nonsolvent) (≥80 vol %) was added to the THF solutions (Scheme 1S). As exemplified by the images in Figure 6c, the differences in emission were obvious between the star polymer and cross-linker TPE-2St in THF solutions with 0 and 50 vol % nonsolvent (*n*-hexane or water) fractions. The reason for the nonemission of TPE-2St in dilute THF solutions is the active intramolecular rotations of the TPE components. In the case of PE stars, the core cross-linked structure restricts the intramolecular rotation which forcefully blocked the nonradiative path and activated radiative decay, resulting in the emission enhancement of the star polymer in dilute solutions. As for the

DOI: 10.1021/acs.macromol.7b00506
Macromolecules XXXX, XXX, XXX−XXX

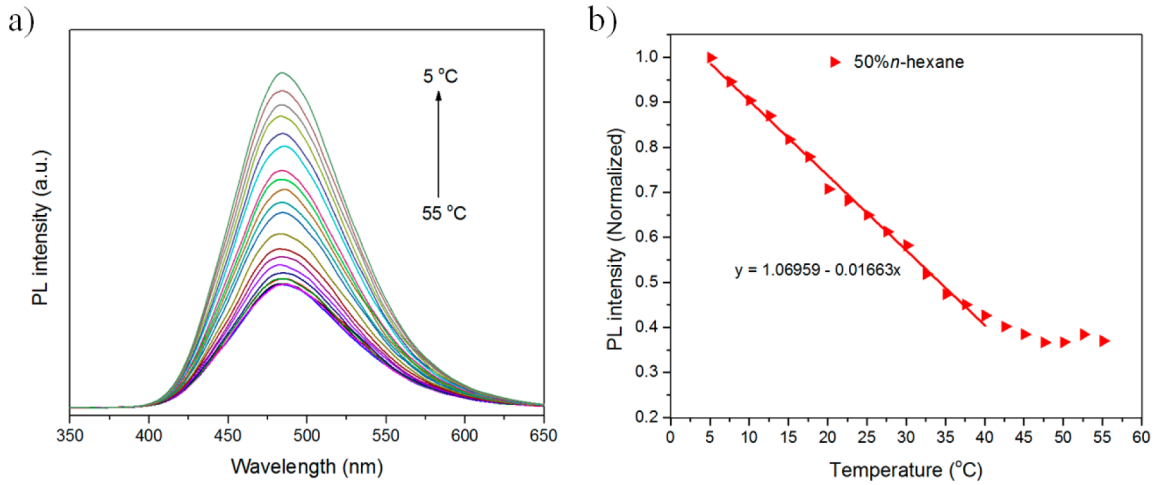

Figure 7. (a) PL spectra of $(PE)_{136}$-P(TPE-2St) in 50/50 vol % THF/*n*-hexane mixture at a concentration of 0.1 g/L with temperature decreasing from 55 to 5 °C by a step size of 2.5 °C. (b) Plot of normalized PL intensity versus temperature, I (5 °C) = 1.0.

aggregate state that we can see from Figure 6d, the solid powder of $(PE)_{136}$-P(TPE-2St) was white color in appearance under normal room lighting within the lab, but emitted a strong greenish-blue light under UV irradiation at 365 nm.

For other star polymers $(PS)_n$-P(TPE-2St) and (TBDMSO-PE-*b*-PCL)$_n$-P(TPE-2St), they showed the emission in dilute THF solutions and addition of water to their THF solution also resulted in a rapid increase of PL intensities (Figure S10 and S11). The rubbery structure played a key role for their luminescent properties especially in dilute solutions, although these polymers possess different kinds of arms.

Temperature Response. Next, the photoluminescence of $(PE)_{136}$-P(TPE-2St) star polymer in 50/50 vol % of THF/*n*-hexane mixture was investigated under varying temperatures (Figure 7). Interestingly, PL intensity increased when decreasing the temperature of the mixture from 47.5 to 5 °C, but remained almost unchanged from 55 to 47.5 °C. Notably, within the responsive window of 40−5 °C, apparent linear relationship of PL intensity versus temperature was observed. The same linear decrease also occurred with another sample $(PE)_{262}$-P(TPE-2St) star polymer in THF/*n*-hexane with 50 or 70 vol % *n*-hexane fraction (Figure S12). A similar phenomenon was reported by Zhao et al. for poly(*N*-isopropylacrylamide) (PNIPAM)-based core/shell hydrogel nanoparticles, and their red-emission rare-earth complex and blue-emission quaternary ammonium tetraphenylethylene derivative (d-TPE), which also exhibited a linear temperature response in the range from 10 to 80 °C.[55] They ascribed such a behavior to the shrinkage of the shell with a temperature decrease, which led to the inhibition of intramolecular rotations and vibrations of d-TPE molecules. The inhibition of intramolecular motions enhanced the PL emission. In our case, due to the nearly spherical shape,[56] TPE molecules may have experienced a shrinkage of arms and be immobilized at low temperature (5−45 °C) similar to the core/shell hydrogel nanoparticles. At a high temperature (47.5−55 °C), the star polymer may have relaxed and intramolecular motions of TPE favored at the same level resulting in the almost same PL emission.

CONCLUSION

In summary, core cross-linked multiarm star polymers with PS, PE, or PE-*b*-PCL arms were synthesized via the "arm-first" strategy by ATRP of the corresponding macroinitiators with AIE TPE-2St, used as a cross-linker. Polyhomologation was utilized for the synthesis of PE-based macroinitiators. All synthesized star polymers exhibited AIE-characters either in bulk or in solution. The emission of these polymers in dilute solutions is caused by the restriction of the intramolecular rotation induced by the core cross-linked structure. Because of their nearly spherical shape, the star polymers exhibited temperature responsive emission in THF/*n*-hexane mixtures, which increasing linearly with decreasing temperature from 40 to 5 °C. We hope the presented results will open new horizons toward a variety of novel luminescent core cross-linked star polymers. Further research on pH-responsive core cross-linked miktoarm stars is underway.

ASSOCIATED CONTENT

Supporting Information

The Supporting Information is available free of charge on the ACS Publications website at DOI: 10.1021/acs.macromol.7b00506.

Figure S1−S12 showing NMR, GPC, DSC, and photoluminescence (PDF)

AUTHOR INFORMATION

Corresponding Author

*(N.H.) Telephone: + 966-(0)12-8080789. E-mail: nikolaos.hadjichristidis@kaust.edu.sa.

ORCID

Panayiotis Bilalis: 0000-0002-5809-9643
Yves Gnanou: 0000-0001-6253-7856
Nikos Hadjichristidis: 0000-0003-1442-1714

Present Address

[§]College of Science, Shantou University, Shantou, Guangdong, 515063 P. R. China.

Notes

The authors declare no competing financial interest.

ACKNOWLEDGMENTS

Research reported in this publication was supported by King Abdullah University of Science and Technology (KAUST).

DOI: 10.1021/acs.macromol.7b00506
Macromolecules XXXX, XXX, XXX−XXX

REFERENCES

(1) Bredol, M.; Kynast, U.; Ronda, C. Designing Luminescent Materials. *Adv. Mater.* **1991**, *3*, 361−367.
(2) Schmidt, A.; Anderson, M. L.; Armstrong, N. R. Electronic states of vapor deposited electron and hole transport agents and luminescent materials for light-emitting diodes. *J. Appl. Phys.* **1995**, *78*, 5619−5625.
(3) Jüstel, T.; Nikol, H.; Ronda, C. New Developments in the Field of Luminescent Materials for Lighting and Displays. *Angew. Chem., Int. Ed.* **1998**, *37*, 3084−3103.
(4) Bünzli, J.-C. G. Lanthanide Luminescence for Biomedical Analyses and Imaging. *Chem. Rev.* **2010**, *110*, 2729−2755.
(5) Förster, T. K.; Kasper, K. Ein Konzentrationsumschlag der Fluoreszenz. *Z. Phys. Chem. (Muenchen, Ger.)* **1954**, *1*, 275−277.
(6) Luo, J.; Xie, Z.; Lam, J. W.; Cheng, L.; Chen, H.; Qiu, C.; Kwok, H. S.; Zhan, X.; Liu, Y.; Zhu, D.; et al. Aggregation-induced emission of 1-methyl-1, 2, 3, 4, 5-pentaphenylsilole. *Chem. Commun.* **2001**, *18*, 1740−1741.
(7) Tang, B. Z. Z.; Zhan, X.; Yu, G.; Sze Lee, P. P.; Liu, Y.; Zhu, D. D., Efficient blue emission from siloles. *J. Mater. Chem.* **2001**, *11*, 2974−2978.
(8) Mei, J.; Hong, Y.; Lam, J. W. Y.; Qin, A.; Tang, Y.; Tang, B. Z. Aggregation-Induced Emission: The Whole Is More Brilliant than the Parts. *Adv. Mater.* **2014**, *26*, 5429−5479.
(9) Kwok, R. T.; Leung, C. W.; Lam, J. W.; Tang, B. Z. Biosensing by luminogens with aggregation-induced emission characteristics. *Chem. Soc. Rev.* **2015**, *44*, 4228−4238.
(10) Mei, J.; Leung, N. L.; Kwok, R. T.; Lam, J. W.; Tang, B. Z. Aggregation-induced emission: together we shine, united we soar! *Chem. Rev.* **2015**, *115*, 11718−11940.
(11) Qin, A.; Lam, J. W.; Tang, B. Z. Luminogenic polymers with aggregation-induced emission characteristics. *Prog. Polym. Sci.* **2012**, *37*, 182−209.
(12) Hu, R.; Kang, Y.; Tang, B. Z. Recent advances in AIE polymers. *Polym. J.* **2016**, *48*, 359−370.
(13) Lai, C.-T.; Chien, R.-H.; Kuo, S.-W.; Hong, J.-L. Tetraphenylthiophene-Functionalized Poly(N-isopropylacrylamide): Probing LCST with Aggregation-Induced Emission. *Macromolecules* **2011**, *44*, 6546−6556.
(14) Yin, X.; Meng, F.; Wang, L. Thermosensitivity and luminescent properties of new tetraphenylethylene derivatives bearing peripheral oligo(ethylene glycol) chains. *J. Mater. Chem. C* **2013**, *1*, 6767−6773.
(15) Liu, T.; Meng, Y.; Wang, X.; Wang, H.; Li, X. Unusual strong fluorescence of a hyperbranched phosphate: discovery and explanations. *RSC Adv.* **2013**, *3*, 8269−8275.
(16) Dong, R.; Zhu, B.; Zhou, Y.; Yan, D.; Zhu, X. Reversible photoisomerization of azobenzene-containing polymeric systems driven by visible light. *Polym. Chem.* **2013**, *4*, 912−915.
(17) Yuan, W. Z.; Zhao, H.; Shen, X. Y.; Mahtab, F.; Lam, J. W. Y.; Sun, J. Z.; Tang, B. Z. Luminogenic Polyacetylenes and Conjugated Polyelectrolytes: Synthesis, Hybridization with Carbon Nanotubes, Aggregation-Induced Emission, Superamplification in Emission Quenching by Explosives, and Fluorescent Assay for Protein Quantitation. *Macromolecules* **2009**, *42*, 9400−9411.
(18) Liu, J.; Zhong, Y.; Lam, J. W. Y.; Lu, P.; Hong, Y.; Yu, Y.; Yue, Y.; Faisal, M.; Sung, H. H. Y.; Williams, I. D.; Wong, K. S.; Tang, B. Z. Hyperbranched Conjugated Polysiloles: Synthesis, Structure, Aggregation-Enhanced Emission, Multicolor Fluorescent Photopatterning, and Superamplified Detection of Explosives. *Macromolecules* **2010**, *43*, 4921−4936.
(19) Liu, J.; Zhong, Y.; Lu, P.; Hong, Y.; Lam, J. W. Y.; Faisal, M.; Yu, Y.; Wong, K. S.; Tang, B. Z. A superamplification effect in the detection of explosives by a fluorescent hyperbranched poly(silylenephenylene) with aggregation-enhanced emission characteristics. *Polym. Chem.* **2010**, *1*, 426−429.
(20) Taniguchi, R.; Yamada, T.; Sada, K.; Kokado, K. Stimuli-Responsive Fluorescence of AIE Elastomer Based on PDMS and Tetraphenylethene. *Macromolecules* **2014**, *47*, 6382−6388.
(21) Hu, R.; Leung, N. L. C.; Tang, B. Z. AIE macromolecules: syntheses, structures and functionalities. *Chem. Soc. Rev.* **2014**, *43*, 4494−4562.
(22) Zhao, W.; Li, C.; Liu, B.; Wang, X.; Li, P.; Wang, Y.; Wu, C.; Yao, C.; Tang, T.; Liu, X.; Cui, D. A New Strategy To Access Polymers with Aggregation-Induced Emission Characteristics. *Macromolecules* **2014**, *47*, 5586−5594.
(23) Li, Y.; Yu, H.; Qian, Y.; Hu, J.; Liu, S. Amphiphilic Star Copolymer-Based Bimodal Fluorogenic/Magnetic Resonance Probes for Concomitant Bacteria Detection and Inhibition. *Adv. Mater.* **2014**, *26*, 6734−6741.
(24) Zhao, Y.; Zhu, W.; Wu, Y.; Qu, L.; Liu, Z.; Zhang, K. An aggregation-induced emission star polymer with pH and metal ion responsive fluorescence. *Polym. Chem.* **2016**, *7*, 6513−6520.
(25) Gao, H.; Matyjaszewski, K. Structural Control in ATRP Synthesis of Star Polymers Using the Arm-First Method. *Macromolecules* **2006**, *39*, 3154−3160.
(26) Gao, H.; Matyjaszewski, K. Arm-First Method As a Simple and General Method for Synthesis of Miktoarm Star Copolymers. *J. Am. Chem. Soc.* **2007**, *129*, 11828−11834.
(27) Xia, J.; Zhang, X.; Matyjaszewski, K. Synthesis of Star-Shaped Polystyrene by Atom Transfer Radical Polymerization Using an "Arm First" Approach. *Macromolecules* **1999**, *32*, 4482−4484.
(28) Connal, L. A.; Li, Q.; Quinn, J. F.; Tjipto, E.; Caruso, F.; Qiao, G. G. pH-Responsive Poly(acrylic acid) Core Cross-Linked Star Polymers: Morphology Transitions in Solution and Multilayer Thin Films. *Macromolecules* **2008**, *41*, 2620−2626.
(29) Du, J.; Chen, Y. PCL Star Polymer, PCL-PS Heteroarm Star Polymer by ATRP, and Core-Carboxylated PS Star Polymer Thereof. *Macromolecules* **2004**, *37*, 3588−3594.
(30) Wiltshire, J. T.; Qiao, G. G. Selectively Degradable Core Cross-Linked Star Polymers. *Macromolecules* **2006**, *39*, 9018−9027.
(31) Baek, K.-Y.; Kamigaito, M.; Sawamoto, M. Star-Shaped Polymers by Metal-Catalyzed Living Radical Polymerization. 1. Design of Ru(II)-Based Systems and Divinyl Linking Agents. *Macromolecules* **2001**, *34*, 215−221.
(32) Liu, P.; Landry, E.; Ye, Z.; Joly, H.; Wang, W.-J.; Li, B.-G. Arm-First" Synthesis of Core-Cross-Linked Multiarm Star Polyethylenes by Coupling Palladium-Catalyzed Ethylene "Living" Polymerization with Atom-Transfer Radical Polymerization. *Macromolecules* **2011**, *44*, 4125−4139.
(33) Zhang, K.; Ye, Z.; Subramanian, R. A Trinuclear Pd−Diimine Catalyst for "Core-First" Synthesis of Three-Arm Star Polyethylenes via Ethylene "Living" Polymerization. *Macromolecules* **2009**, *42*, 2313−2316.
(34) Zhang, Y.; Ye, Z. Covalent Surface Grafting of Branched Polyethylenes on Silica Nanoparticles by Surface-Initiated Ethylene "Living" Polymerization with Immobilized Pd−Diimine Catalysts. *Macromolecules* **2008**, *41*, 6331−6338.
(35) Luo, J.; Shea, K. J. Polyhomologation. A Living C1 Polymerization. *Acc. Chem. Res.* **2010**, *43*, 1420−1433.
(36) Shea, K. J.; Walker, J. W.; Zhu, H.; Paz, M.; Greaves, J. Polyhomologation. A Living Polymethylene Synthesis. *J. Am. Chem. Soc.* **1997**, *119*, 9049−9050.
(37) Wagner, C. E.; Shea, K. J. 1-Boraadamantane Blows Its Top, Sometimes. The Mono- and Polyhomologation of 1-Boraadamantane. *Org. Lett.* **2001**, *3*, 3063−3066.
(38) Luo, J.; Zhao, R.; Shea, K. J. Synthesis of High Molecular Weight Polymethylene via C1 Polymerization. The Role of Oxygenated Impurities and Their Influence on Polydispersity. *Macromolecules* **2014**, *47*, 5484−5491.
(39) Zhang, H.; Hadjichristidis, N. Well-Defined Bilayered Molecular Cobrushes with Internal Polyethylene Blocks and ω-Hydroxyl-Functionalized Polyethylene Homobrushes. *Macromolecules* **2016**, *49*, 1590−1596.
(40) Zhang, H.; Zhang, Z.; Gnanou, Y.; Hadjichristidis, N. Well-Defined Polyethylene-Based Random, Block, and Bilayered Molecular Cobrushes. *Macromolecules* **2015**, *48*, 3556−3562.

DOI: 10.1021/acs.macromol.7b00506
Macromolecules XXXX, XXX, XXX−XXX

(41) Zhang, Z.; Zhang, H.; Gnanou, Y.; Hadjichristidis, N. Polyhomologation based on in situ generated boron-thexyl-silaboracyclic initiating sites: a novel strategy towards the synthesis of polyethylene-based complex architectures. *Chem. Commun.* **2015**, *51*, 9936−9938.
(42) Zhang, Z.; Altaher, M.; Zhang, H.; Wang, D.; Hadjichristidis, N. Synthesis of Well-Defined Polyethylene-Based 3-Miktoarm Star Copolymers and Terpolymers. *Macromolecules* **2016**, *49*, 2630−2638.
(43) Zhang, Z.; Gnanou, Y.; Hadjichristidis, N. Well-defined 4-arm stars with hydroxy-terminated polyethylene, polyethylene-b-polycaprolactone and polyethylene-b-(polymethyl methacrylate) 2 arms. *Polym. Chem.* **2016**, *7*, 5507−5511.
(44) Corey, E. J.; Chaykovsky, M. Dimethyloxosulfonium Methylide ((CH3)2SOCH2) and Dimethylsulfonium Methylide ((CH3)-2SCH2). Formation and Application to Organic Synthesis. *J. Am. Chem. Soc.* **1965**, *87*, 1353−1364.
(45) Matyjaszewski, K.; Patten, T. E.; Xia, J. Controlled/"Living" Radical Polymerization. Kinetics of the Homogeneous Atom Transfer Radical Polymerization of Styrene. *J. Am. Chem. Soc.* **1997**, *119*, 674−680.
(46) Guan, W.; Zhou, W.; Lu, C.; Tang, B. Z. Synthesis and Design of Aggregation-Induced Emission Surfactants: Direct Observation of Micelle Transitions and Microemulsion Droplets. *Angew. Chem., Int. Ed.* **2015**, *54*, 15160−15164.
(47) Peng, Q.; Yi, Y.; Shuai, Z.; Shao, J. Toward Quantitative Prediction of Molecular Fluorescence Quantum Efficiency: Role of Duschinsky Rotation. *J. Am. Chem. Soc.* **2007**, *129*, 9333−9339.
(48) Tseng, N.-W.; Liu, J.; Ng, J. C. Y.; Lam, J. W. Y.; Sung, H. H. Y.; Williams, I. D.; Tang, B. Z. Deciphering mechanism of aggregation-induced emission (AIE): Is E-Zisomerisation involved in an AIE process? *Chem. Sci.* **2012**, *3*, 493−497.
(49) Liang, G.; Lam, J. W. Y.; Qin, W.; Li, J.; Xie, N.; Tang, B. Z. Molecular luminogens based on restriction of intramolecular motions through host-guest inclusion for cell imaging. *Chem. Commun.* **2014**, *50*, 1725−1727.
(50) Zhao, J.; Yang, D.; Zhao, Y.; Yang, X.-J.; Wang, Y.-Y.; Wu, B. Anion-Coordination-Induced Turn-On Fluorescence of an Oligourea-Functionalized Tetraphenylethene in a Wide Concentration Range. *Angew. Chem., Int. Ed.* **2014**, *53*, 6632−6636.
(51) Shi, J.; Chang, N.; Li, C.; Mei, J.; Deng, C.; Luo, X.; Liu, Z.; Bo, Z.; Dong, Y. Q.; Tang, B. Z. Locking the phenyl rings of tetraphenylethene step by step: understanding the mechanism of aggregation-induced emission. *Chem. Commun.* **2012**, *48*, 10675−10677.
(52) Liu, Y.; Zhao, Z.; Lam, J. W. Y.; Zhao, Y.; Chen, Y.; Liu, Y.; Tang, B. Z. Cascade Polyannulation of Diyne and Benzoylacetonitrile: A New Strategy for Synthesizing Functional Substituted Poly(naphthopyran)s. *Macromolecules* **2015**, *48*, 4241−4249.
(53) Mullin, J. L.; Tracy, H. J.; Ford, J. R.; Keenan, S. R.; Fridman, F. Characteristics of Aggregation Induced Emission in 1,1-Dimethyl-2,3,4,5-tetraphenyl and 1,1,2,3,4,5-Hexaphenyl Siloles and Germoles. *J. Inorg. Organomet. Polym. Mater.* **2007**, *17*, 201−213.
(54) Valeur, B.; Berberan-Santos, M. N. *Molecular fluorescence: principles and applications*.; John Wiley & Sons: 2012.
(55) Zhao, Y.; Shi, C.; Yang, X.; Shen, B.; Sun, Y.; Chen, Y.; Xu, X.; Sun, H.; Yu, K.; Yang, B.; Lin, Q. pH- and Temperature-Sensitive Hydrogel Nanoparticles with Dual Photoluminescence for Bioprobes. *ACS Nano* **2016**, *10*, 5856−5863.
(56) Snijkers, F.; Cho, H. Y.; Nese, A.; Matyjaszewski, K.; Pyckhout-Hintzen, W.; Vlassopoulos, D. Effects of Core Microstructure on Structure and Dynamics of Star Polymer Melts: From Polymeric to Colloidal Response. *Macromolecules* **2014**, *47*, 5347−5356.

DOI: 10.1021/acs.macromol.7b00506
Macromolecules XXXX, XXX, XXX−XXX